NASA TECHNICAL MEMORANDUM

NASA TM X-52729

NASA TM X-52729

THE COMPRESSIBLE FLOW OF TWO COMPONENT, TWO-PHASE MIXTURES IN NOZZLES AND ORIFICES

by Robert E. Henry
Lewis Research Center
Cleveland, Ohio

TECHNICAL PAPER proposed for presentation at
1970 Heat Transfer and Fluid Mechanics Institute
U. S. Naval Postgraduate School
Monterey, California, June 10-12, 1970

THE COMPRESSIBLE FLOW OF TWO COMPONENT, TWO-PHASE MIXTURES IN NOZZLES AND ORIFICES

by Robert E. Henry

Lewis Research Center
Cleveland, Ohio

TECHNICAL PAPER proposed for presentation at

1970 Heat Transfer and Fluid Mechanics Institute
U. S. Naval Postgraduate School, Monterey, California, June 10-12, 1970

NATIONAL AERONAUTICS AND SPACE ADMINISTRATION

THE COMPRESSIBLE FLOW OF TWO COMPONENT, TWO-PHASE MIXTURES IN NOZZLES AND ORIFICES

Robert E. Henry*

ABSTRACT

The critical discharge of two-component, two-phase mixtures through convergent nozzles is analytically investigated for initially dispersed or annular-dispersed flow patterns. The processes of interphase heat and momentum transfer are considered, and based on the experimental results of previous investigators, credible assumptions are made for these processes. The resulting model yields predictions for both the critical pressure ratio and flow rate as a function of the stagnation conditions. The analytical results exhibit good agreement with the published air-water nozzle data.

The model is extended to compressible flows through orifices and nozzles and again exhibits good agreement with the available two-component data.

E-5440

INTRODUCTION

The compressible flow of two-phase mixtures has received considerable attention because of its occurrence in such problems as the blowdown of reactor pressure vessels [1], the venting of rocket propellant tanks [2], the design of jet pumps [3], and the metering and control of two-phase flow [4]. Generally, the practical problem involves the flow of a one-component mixture, however, much information about such flows can be obtained from observing the behavior of two-component mixtures. For example, several experimental studies have employed air-water mixtures to observe the interphase processes of heat and momentum transfer. This information is extremely difficult to extract from one-component flows because of the simultaneously occurring mass transfer process.

The objective of this investigation is to closely examine the available air-water nozzle data and employ this information to construct a compressible flow model which incorporates reasonable approximations for the rates and amounts of interphase heat and momentum transfer. The result will be a useful guide in structuring a mathematical model for one-component, two-phase compressible flows.

ANALYSIS

The steady-state, one-dimensional, continuity and momentum equations for two-component (x = constant) flows can be written as

Liquid Continuity

$$W_l v_l = A_l u_l \tag{1}$$

*NASA Lewis Research Center, Cleveland, Ohio

Gas Continuity

$$W_g v_g = A_g u_g \tag{2}$$

Momentum

$$- A \frac{dP}{dZ} = W_g \frac{du_g}{dZ} + W_l \frac{du_l}{dZ} + \frac{dF_w}{dZ} + \frac{d\theta}{dZ} \tag{3}$$

For the high velocities characteristic of critical flow, the frictional and hydrostatic head loss quantities can be neglected with respect to the inertial and pressure gradient terms. For simplicity only isolated systems are considered.

Equation 3 can be approximated by

$$- \frac{dP}{dZ} = G\left[x \frac{du_g}{dZ} + (1 - x) \frac{du_l}{dZ}\right] \tag{4}$$

It is assumed that, for fixed stagnation conditions, u_g and u_l are of the form $f[P(Z)]$. Hence, Eq. 4 shows

$$G_t^{-1} = -\left[x \frac{du_g}{dP} + (1 - x) \frac{du_l}{dP}\right]_t \tag{5}$$

(The subscript t indicates that all the enclosed quantities are evaluated at the throat.) The critical flow criterion states that for fixed stagnation conditions, the flow rate exhibits a maximum with respect to the throat pressure.

$$\left.\frac{dG}{dP}\right)_t = 0 \tag{6}$$

If k is defined by

$$k = \frac{u_g}{u_l} = \frac{x}{1 - x} \frac{1 - \alpha}{\alpha} \frac{v_g}{v_l} \tag{7}$$

the critical criterion can be applied to Eq. 5 to give:

$$G_c^2 = -\left(k \left\{ [1 + x(k - 1)]x \frac{dv_g}{dP} + k[1 + x(k - 2) - x^2(k - 1)] \right.\right.$$

$$\left.\left. \frac{dv_l}{dP} + x(1 - x)\left(kv_l - \frac{v_g}{k}\right) \frac{dk}{dP} \right\}^{-1} \right)_t \tag{8}$$

For all but the extremely small qualities (x of order 10^{-5}), the role of the liquid compressibility can be neglected, hence, the liquid phase is considered to be incompressible.

The term $(dv_g/dP)_t$ represents the compressibility of the gaseous phase and may be expressed as $(dv_g/dZ)_t/(dP/dZ)_t$. If it is assumed that the gas is perfect ($Pv_g = RT_g$) then,

$$\frac{(dv_g/dZ)_t}{(dP/dZ)_t} = -\left\{\frac{v_g}{P}\left[1 - \frac{P}{T_g}\left(\frac{dT_g/dZ}{dP/dZ}\right)\right]\right\}_t \qquad (9)$$

Therefore, to describe the compressibility at the throat one must describe the axial temperature gradient which is indicative of the interphase heat transfer rate. Smith, et al. [5] measured axial temperature profiles of a liquid film in the dispersed-annular critical flow of air-water mixtures through an annular venturi. These profiles are shown in Fig. 1.

Smith purposely generated a liquid film on the straight wall (Fig. 1) upstream of the convergent region. Photographs show that this wall film persists through the convergent and throat regions and into the divergent region. The schlieren photograph of compressible gas-particle flows presented by Gilbert, et al. [6] also suggest that the more dense phase is concentrated near the centerline in the throat vicinity. (For Smith's geometry, the centerline would be equivalent to the straight wall.) Such preferential distributions are in agreement with what one would expect from the two-dimensional flow field in the throat vicinity. Based on these observations, a flow pattern development like that shown in Fig. 2 is assumed to be typical of convergent nozzle flows, and, thus, Smith's results can be considered to be representative of all such flows. This flow pattern structure is only proposed for flows in which the inlet pattern is annular, annular-dispersed, or mist and not for bubbly mixtures like those observed by Muir and Eichhorn [7].

Table I compares the measured stagnation to throat temperature drops shown in Fig. 1 to the predictions of the thermal equilibrium model which assumes the gas and liquid temperatures are equal at all times. If the gas expansion is represented by a polytropic process ($Pv_g^{n_E}$ = constant), the thermal equilibrium assumption gives

$$n_E = \frac{(1 - x)c_l + xc_p}{(1 - x)c_l + xc_v} \qquad (10)$$

This is the same formulation derived by Tangren, et al.[8]. Table I also includes measurements reported by Vogrin [9] for temperature differences between the two stations shown in Fig. 3. The accompanying radial void fraction profiles reported in reference 9 indicate that the downstream measurement is representative of a liquid wall film. Therefore, the measurements are interpreted in the same manner as those of reference 5. The data given in Table I and Fig. 1 show the liquid temperature is essentially constant throughout these rapid expansions. Thus, there is no significant amount of heat exchanged with the gaseous phase which, therefore, expands in an adiabatic manner. However, the temperature profiles of Fig. 1 show a large temperature gradient at the throat, hence, the rate of change is quite different from an adiabatic process. If it is assumed that, for a given phase distribution, the rate of interphase heat transfer is proportional to the temperature difference between the phases:

$$q = hA_s(T_l - T_g) \tag{11}$$

The amount of heat transferred in the expansion is the rate integrated over the time necessary for the mixture to travel from the stagnation region to the throat.

$$Q = \int_o^\tau q\, dt \tag{12}$$

Figure 2 shows the one-dimensional pressure profile for a typical nozzle configuration. In the convergent portion, the acceleration and the accompanying steep pressure gradients occur between the upstream location which has a diameter twice that of the throat and the throat itself. The temperature profiles, which are based on the results of reference 5, show that where times are long (low velocity), the temperature difference is small and that where the temperature difference is appreciable, the residence time is short (high velocity). Therefore, it is assumed that the expansion is so rapid that the amount of heat transferred is negligible ($Q \approx 0$).

$$P_o v_{go}^{\gamma} = P_t v_{gt}^{\gamma} \tag{13}$$

Figure 2 also shows that the rate of heat transfer at the throat can be quite large. If it is assumed that the gaseous behavior in the throat region can be represented by another polytropic process ($Pv_g^{n_t} = \text{constant}$), the exponent n_t must reflect a sizable heat transfer rate and, thus, cannot be equal to the isentropic exponent γ. As a compromise between simplicity and the real process, it is assumed that n_t is equal to the equilibrium exponent (n_E) given in Eq. 10, which is indicative of a large rate of interphase heat transfer.

$$\frac{dv_{gt}}{dP_t} = -\frac{v_{gt}}{n_E P_t} \tag{14}$$

The above arguments have essentially separated the expansion into two parts such that one approximation can be made for the overall expansion and another for the rate process at the throat.

To evaluate the critical flow rate, it is necessary to describe the derivative $dk/dP)_t$ which is representative of the interphase momentum transfer rate. Using the axial void fraction measurements of Vogrin and the approximation given in Eq. 13, one can calculate the velocity ratio profiles shown in Fig. 3. Since the velocity ratio is assumed to be of the form $k[P(z)]$,

$$\left.\frac{dk}{dP}\right)_t = \frac{dk/dz)_t}{dP/dz)_t} \tag{15}$$

Figure 3 shows $dk/dz)_t$ is either zero (a minimum) or small (k nearly constant) while $dP/dz)_t$ is quite large. As a first approximation it is assumed that

$$\left.\frac{dk}{dP}\right)_t = 0 \tag{16}$$

for nozzle flows operating in the annular, annular-dispersed, or mist flow ranges.

The approximations given in Eqs. 14 and 16 and the incompressible liquid assumption ($dv_l/dP = 0$) enable one to simplify Eq. 8 to:

$$G_c^2 = \left\{\frac{kn_E P}{[1 + x(k - 1)]xv_g}\right\}_t \tag{17}$$

If the velocity ratio is assumed constant throughout the expansion, the two-phase frictionless momentum equation (Eq. 4) can be written as

$$-\frac{k[(1 - x)v_l + xv_g]}{1 + x(k - 1)}\,dP = d\left(\frac{u_g^2}{2}\right) \tag{18}$$

Using the assumption given in Eq. 13, along with Eq. 17, this expression can be integrated between the stagnation and throat locations to give:

$$(1 - x)kv_l(P_o - P_t) + \frac{x\gamma}{\gamma - 1}(P_o v_{go} - P_t v_{gt})$$

$$= \left\{[(1 - x)kv_l + xv_g]^2 \frac{n_E P}{2xv_g}\right\}_t \tag{19}$$

Equation 19 can be rearranged and expressed more compactly as:

$$\eta = \frac{\frac{1 - \alpha_t}{\alpha_t} + \frac{\gamma}{\gamma - 1}\eta^{1/\gamma}}{\left[\frac{n_E}{2\alpha_t^2} + \frac{(1 - \alpha_t)}{\alpha_t} + \frac{\gamma}{\gamma - 1}\right]} \tag{20}$$

where

$$\eta = \frac{P_t}{P_o} \tag{21}$$

The constant velocity ratio assumption is obviously not in agreement with the axial profiles shown in Fig. 3. However, the high upstream velocity ratios shown occur in the stagnation region where system velocities are negligible and the velocity ratio is essentially meaningless. The assumption implies the velocity ratio is essentially constant in the region of high acceleration. A similar assumption has been widely used for particulate compressible flows [10].

Since the constant velocity ratio assumption dictates that

$$\alpha_o = \frac{\alpha_t \eta^{1/\gamma}}{1 - \alpha_t(1 - \eta^{1/\gamma})} \tag{22}$$

the critical pressure ratio is only a function of either the stagnation or throat void fraction and the polytropic exponents γ and n_E. Figure 4 compares the proposed model and the thermal equilibrium solution with the experimental results of ref. 9 as a function of stagnation and throat void fractions. It is seen that there is little difference between the two solutions, however, of the two models, the one proposed herein appears to be more characteristic of the data.

Unfortunately, the void fraction is usually unknown, and, thus, it is preferable to express the critical pressure ratio as a function of quality. As shown by Eq. 19, such an expression requires a knowledge of the throat velocity ratio. These velocity ratios can be calculated for Vogrin's experiment by using the measured throat void fractions and the adiabatic expansion assumption discussed above. The values, as shown in Fig. 5, appear to exhibit some pressure dependency, however, the uncertainty is so large that any attempt to discern such a relationship would be highly speculative. Therefore, as a first approximation, it is assumed that the velocity ratio is dependent upon neither the pressure nor the quality and equal to the average of the data shown ($k_t = 3.2$). Equation 20 can be written as

$$\eta = \frac{\frac{(1 - x)k_t v_l}{x v_{gt}} + \frac{\gamma}{\gamma - 1}\eta^{1/\gamma}}{\frac{n_E}{2}\left[\frac{(1 - x)k_t v_l}{x v_{gt}} + 1\right]^2 + \left[\frac{(1 - x)k_t v_l}{x v_{gt}}\right] + \frac{\gamma}{\gamma - 1}} \tag{23}$$

where

$$v_{gt} = \frac{RT_o}{P_o}(\eta^{-1/\gamma}) \tag{24}$$

and the critical flow relation is given by

$$G_c^2 = \frac{k_t n_E P_o^2 \eta^{(\gamma+1)/\gamma}}{[1 + x(k_t - 1)]xRT_o} \tag{25}$$

For given conditions of x, T_o, and either the stagnation or throat pressure, the transcendental critical pressure ratio expression can be solved. This solution implicitly involves the critical flow rate, thus, a solution of Eq. 23 yields values for the critical pressure ratio and mass flow rate.

In summary a model is proposed for the critical flow of a two-component mixture which is initially in an annular, annular-dispersed, or mist flow configuration. The model varies from

those existing in the literature because it employs separate assumptions for the amounts of heat and momentum transferred in the expansion and the rates of these interphase processes occurring at the throat. The proposed one-dimensional solution is dependent on the throat velocity ratio and is somewhat limited by the lack of experimental measurements of this quantity.

COMPARISON WITH EXPERIMENTAL RESULTS

It is convenient to nondimensionalize the critical flow rate with the prediction of the well documented Homogeneous Thermal Equilibrium Model. This model is presented in ref. 8 and is based on the following assumptions:

1. The average velocities of the phases are equal ($k = 1$) at all times.

2. Thermal equilibrium exists between the phases ($T_g = T_l$) at all times.

3. The system entropy is constant.

The critical pressure ratio and flow rate predictions for this model are given by:

$$\eta_{HE} = \frac{\frac{(1 - x)v_l}{xv_{gH}} + \frac{r_E}{n_E - 1}\eta_{HE}^{1/n_E}}{\frac{n_E}{2}\left[\frac{(1 - x)v_l}{xv_{gH}} + 1\right]^2 + \left[\frac{(1 - x)v_l}{xv_{gH}}\right] + \frac{n_E}{n_E - 1}} \tag{26}$$

and

$$G_{cH}^2 = \frac{n_E P_o^2}{xRT_o}\left[\eta_{HE}^{(n_E+1)/n_E}\right] \tag{27}$$

where

$$v_{gH} = \frac{RT_o}{P_o}\left(\eta_{HE}^{-1/n_E}\right) \tag{28}$$

Dividing Eq. 25 by Eq. 27 gives

$$\frac{G_c}{G_{cH}} = \left\{\frac{k_t \eta^{(\gamma+1)/\gamma}}{[1 + x(k_t - 1)]\left[\eta_{HE}^{(n_E+1)/n_E}\right]}\right\}^{1/2} \tag{29}$$

This expression is only slightly dependent on pressure and, thus, is a convenient means with which to compare the proposed model and experimental data over a wide range of stagnation pressures.

The critical pressure ratio predictions of Eqs. 23 and 26 are compared to the experimental results of Vogrin and Smith in

Fig. 6. (For all the data and models presented herein, the gaseous phase is assumed to be at 100% relative humidity in the stagnation region and the weight fraction of water vapor remains constant at this value throughout the expansion.) Here again it is seen that there is little difference between the Homogeneous Thermal Equilibrium Model and the proposed solution throughout the quality range considered. However, the data in the low quality region of annular-dispersed flows are generally better described by the proposed model. The discrepancies at the higher qualities are due to the oversimplification of the interphase heat transfer rate at the throat. The prediction of Chisholm [11] is also included to illustrate the sensitivity of these relationships to the values chosen for the polytropic exponents. The solution presented by Chisholm differs from the proposed model in two ways. First, the velocity ratio correlation is formed from the long constant area duct results of Fauske [12], and secondly, the total expansion between the stagnation and throat regions is assumed to be isothermal and the throat polytropic exponent (n_t) is taken to be 1.2. These thermodynamic approximations are essentially the inverse of those made in this study. The critical pressure ratio results given in Fig. 6 are mainly a function of the values chosen for the polytropic exponents, and the available data support the assumptions proposed herein as opposed to those of Chisholm.

Figure 7 compares the normalized flow rate predictions of Eq. 29 and those of Chisholm with the data of Smith and Vogrin. For a stagnation pressure of 30 psia, the predictions of the two models are quite close, however, the Chisholm model exhibits a strong pressure dependency which is not characteristic of the data. The slight pressure dependency given by Eq. 29 is more representative of the experimental results.

By considering Figs. 6 and 7 together, the reader can discern the merits of the proposed model. The Homogeneous Thermal Equilibrium Model yields a good prediction for the critical pressure ratio but it is off by as much as 100% in the flow rate prediction. On the other hand, Chisholm's approach gives a good estimate of the flow rate but an erroneous value for the pressure ratio. Therefore, neither of these two solutions correctly describes the physical phenomenon. The proposed model yields good predictions for both the critical pressure ratio and flow rate and, thus, is more characteristic of the actual behavior.

The geometries of refs. 5 and 9 where similar in that they were both straight wall converging-diverging nozzles. Smith reported results for flows with and without a liquid wall film upstream of the convergent region. The data without a wall film are closer to the upstream flow configuration of Vogrin's data and generally exhibits better agreement with the results of ref. 9. It is expected that the throat velocity ratio is determined by the flow pattern development which is dependent on the nozzle geometry and the inlet flow configuration. The data shown in Figs. 6 and 7 demonstrate that the inlet flow pattern exerts a very small influence on the system compressibility. In contrast, the data of Graham [13], shown in Fig. 8, clearly illustrate the influence of nozzle geometry on the critical flow

rates. (Since Graham exhausted directly to the atmosphere, only runs with stagnation pressures greater than 30 psia are considered. This ensures the results are characteristic of choked flow.) Since each of the geometries reported shows G_c/G_{cHE} to be essentially independent of pressure, it seems reasonable to conclude that the discrepancies between Eq. 29 and the data are a result of the crude approximation given in Fig. 5. When the drastic differences between the test nozzles are considered, it is not surprising that this approximation is not universally valid. The model generally overpredicts the experimental results, however, it does correctly describe the trends with quality and pressure. This gives support to the assumptions employed to represent the amount of heat transfer and the rates of interphase heat and mass transfer at the throat. These assumptions are further justified by comparing the model with the high pressure air-water data of Netzer [14]. Obviously, at high pressures, the throat velocity ratio will be smaller because the density difference between the phases is decreased. Table II compares the data of ref. 14 with the proposed model for throat velocity ratios of 1.0, 1.3 (the approximate value generated by Netzer's numerical analysis), and 3.2. The model shows better agreement for smaller velocity ratios, which is the expected trend, and yields a good prediction for the critical pressure ratio which is only slightly dependent on the throat velocity ratio. Therefore, it is seen that the proposed solution is properly sensitive to the throat velocity ratio, but, as discussed above, it is limited by the lack of throat velocity ratio data as a function of stagnation pressure and nozzle geometry.

For the pressure levels shown in Fig. 8, flows with qualities in the range $0.005 < x < 0.010$ should begin to transition into bubbly flow patterns, and the model is not intended for this type of flow configuration.

EXTENSIONS OF THE ANALYTICAL MODEL

In addition to the experimental results for convergent nozzles, attention has been given to the compressible flow of two-phase, two-component mixtures through orifices and cylindrical nozzles. If the single phase compressible behavior in such geometries is known, the two-phase model developed above can be extended to these configurations.

Perry [15] has experimentally demonstrated that the discharge coefficient for the compressible flow of air through a sharp edged orifice is approximately 0.84. Jobson [16] has analytically shown that this value is consistent with the incompressible coefficient of 0.61. It is assumed here that the single phase compressible value is applicable to two-phase compressible flows. The discharge coefficient for flow from a stagnation condition is defined by

$$C = \frac{\sqrt{2 \int_{P_t}^{P_o} \frac{dP}{\rho}}}{u_t} \qquad (30)$$

This definition alters the critical pressure ratio expression (Eq. 23) to

$$\eta = \frac{\frac{(1 - x)k_t v_l}{x v_{gt}} + \frac{\gamma}{\gamma - 1}\eta^{1/\gamma}}{\frac{n_E}{2C^2}\left[\frac{(1 - x)k_t v_l}{x v_{gt}} + 1\right]^2 + \left[\frac{(1 - x)k_t v_l}{x v_{gt}}\right] + \frac{\gamma}{\gamma - 1}} \qquad (31)$$

This relationship was solved for given conditions of x, T_o, and P_o with $k_t = 3.2$ as shown in Fig. 5. The resulting critical flow rate prediction is compared to the sharp edged orifice data of Graham [13] in Fig. 9. The good agreement between the model and the data is readily apparent. Here again, as the flow regime becomes a bubbly mixture, the proposed model is not expected to be representative of the data.

Guzhov and Medvedev [17] have reported data for the compressible flow of air-water mixtures through cylindrical nozzles (L/D = 4 and 5). The experimental discharge coefficients for single phase compressible flow through such configurations appears to vary from 0.80 to 0.93 [18]. Therefore, as a first approximation, it is assumed that the orifice coefficient, 0.84, is also applicable here. The experimental data presented in [17] are for throat pressures ranging from 17.4 to 23.2 psia. For a basis of comparison, an average throat pressure of 20 psia was chosen for computation. Figures 10 and 11 compare the results of Guzhov and Medvedev with the model proposed in this study. The model describes the data trends very well and exhibits good agreement for $x > 0.004$. This quality is in or near the region of a transition to a bubbly configuration, thus, it is not surprising that the model is not representative of the data for qualities less than 0.004.

SUMMARY AND CONCLUSIONS

A model is developed for the critical discharge of two-component, two-phase dispersed, annular-dispersed, or mist flow mixtures through convergent nozzles. The basic approach emphasizes the need for separate approximations to represent the amount of interphase heat and momentum transfer throughout the expansion and the rates of transfer at the throat.

The proposed solution is superior to those presently in the literature because it yields accurate predictions for both the critical pressure ratio and the critical flow rate. However, the general application of the model is limited by the lack of throat velocity ratio data as a function of the pressure level and nozzle geometry.

Based on the results of single phase flow, the model can be extended to the compressible flow of two-component mixtures through orifices and cylindrical nozzles. A comparison with the available data shows good agreement with the experimental results for such configurations.

NOMENCLATURE

A	area
C	discharge coefficient
c	specific heat
F_W	wall shear
f	function
G	flow rate/unit area
h	heat transfer coefficient
k	velocity ratio u_g/u_l
n	polytropic exponent
P	pressure
Q	heat
q	heat per unit time
R	universal gas constant
T	temperature
t	time
u	velocity
v	specific volume
W	flow rate
x	quality W_g/W_l
Z	axial length
α	void fraction $A_g/(A_g + A_l)$
β	volume fraction
γ	isentropic exponent
η	critical pressure ratio P_t/P_o
θ	hydrostatic head force
ρ	density
τ	transit time between stagnation and throat locations

Subscripts

c	critical flow
E	thermal equilibrium ($T_g = T_l$)
g	gaseous phase
H	homogeneous
l	liquid phase
m	mixture
o	stagnation
p	constant pressure
s	surface
t	throat
v	constant volume

REFERENCES

1. Henry, R. E. "A Study of One- and Two-Component Two-Phase Critical Flows at Low Qualities," Argonne National Laboratory Report ANL-7430, Argonne, Ill.: March 1968.

2. Campbell, H. M., and T. J. Overcamp, "Critical Flowrate of Two-Phase Nitrogen," NASA TM X-53492, Huntsville, Alabama: George C. Marshall Space Flight Center, July 1966.

3. Grolmes, M. A. "Steam-Water Condensing-Injector Performance Analysis With Supersonic Inlet Vapor and Convergent Condensing Section," Argonne National Laboratory Report ANL-7443, Argonne, Ill.: May 1968.

4. Chisholm, D., Flow of Compressible Two-Phase Mixtures Through Throttling Devices, Chem. Process Eng., 1967, 48 (12), 73.

5. Smith, R. V., L. B. Cousins, and G. F. Hewitt "Two-Phase Two-Component Critical Flow in a Venturi," Atomic Energy Research Establishment Report AERE-R5736, Harwell, Berkshire: Chemical Eng. Div., 1968.

6. Gilbert, M., J. Allport, and R. Dunlap. Dynamics of Two-Phase Flow in Rocket Nozzles, ARS J., 1962, 32 (12), 1929-30.

7. Muir, J. F., and R. Eichhorn. Compressible Flow of an Air-Water Mixture Through a Vertical Two-Dimensional, Converging-Diverging Nozzle," p. 183 in Proceedings of 1963 Heat Transfer and Fluid Mechanics Institute. Stanford, Calif.: Stanford Univ. Press, 1963.

8. Tangren, R. F., C. H. Dodge, and H. S. Seifert. Compressibility Effects in Two-Phase Flow, J. Appl. Phys., 1949, 20 (7), 637-45.

9. Vogrin, J. A. "An Experimental Investigation of Two-Phase, Two-Component Flow in a Horizontal Converging-Diverging Nozzle," Argonne National Laboratory Report ANL-6754, Argonne, Ill.: July 1963.

10. Kliegel, J. R. Gas Particle Nozzle Flows, p. 811 in Ninth Symposium (International) on Combustion. New York: Academic Press, 1963.

11. Chisholm, D. Critical Flow Conditions During the Flow of Two-Phase Mixtures Through Nozzles, Proc. Inst. Mech. Engrs., 1968, 182, 145.

12. Fauske, H. K. Two-Phase Two- and One-Component Critical Flow, p. G101 in Proceedings of Symposium on Two-Phase Flow, Univ. of Exeter, Exeter, England, 1965.

13. Graham, E. J. "The Flow of Air-Water Mixtures Through Nozzles," NEL Report No. 308, East Kilbride, Glasgow: Applied Heat Trans. Div., 1967.

14. Netzer, D. W. "Calculations of Flow Characteristics for Two-Phase Flow in Annular Converging-Diverging Nozzles," Purdue Univ. Jet Prop. Center Report TM-62-3. Lafayette, Ind.: The Laboratory, 1962.

15. Perry, J. A. Critical Flow Through Sharp-Edged Orifices, Trans. ASME, 1949, 71, 757-64.

16. Jobson, D. A. On the Flow of a Compressible Fluid Through Orifices, Proc. Inst. Mech. Engrs., 1955, 169, 767-75.

17. Guzhov, A. I., and V. F. Medvedev. Investigation of Gas-Liquid Flow Through Cylindrical Nozzles at Critical Parameters, Thermal Eng., 1966, 13 (8), 117-20.

18. Arnberg, B. T. Review of Critical Flow Meters for Gas Flow Measurements, J. Basic Eng., 1962, 84, 447.

TABLE I. - MEASURED LIQUID TEMPERATURE DROPS IN RAPID EXPANSIONS

Investigator	Quality, x	ΔT (°F) Measured	ΔT (°F) Thermal Equi.
Vogrin	0.0587	0.0	-3.42
	0.0684	+0.5	-4.45
	0.0817	-1.5	-5.76
	0.0891	-0.5	-6.76
Smith, et al.	0.945	-1.5	-55.5
	0.827	-2.0	-45.5

TABLE II. - COMPARISON OF ANALYTICAL MODELS WITH THE EXPERIMENTAL DATA OF NETZER

	P_o (psia)	x	k_t	η	G_c (lbm/sec-ft^2)
Experimental Data	515	0.091	---	0.55	5730
Hom. Ther. Equi. Model	515	0.091	1.0	0.56	4770
Proposed Model	515	0.091	1.0	0.57	5248
	515	0.091	1.3	0.55	5770
	515	0.091	3.2	0 48	7482
Chisholm Model	515	0.091	1.1	C.49	4885
Experimental Data	515	0.130	---	0.57	5050
Hom. Ther. Equi. Model	515	0.130	1.0	0.57	4220
Proposed Model	515	0.130	1.0	0.58	4504
	515	0.130	1.3	0.57	4957
	515	0.130	3.2	0.52	6410
Chisholm Model	515	0.130	1.1	0.50	4190

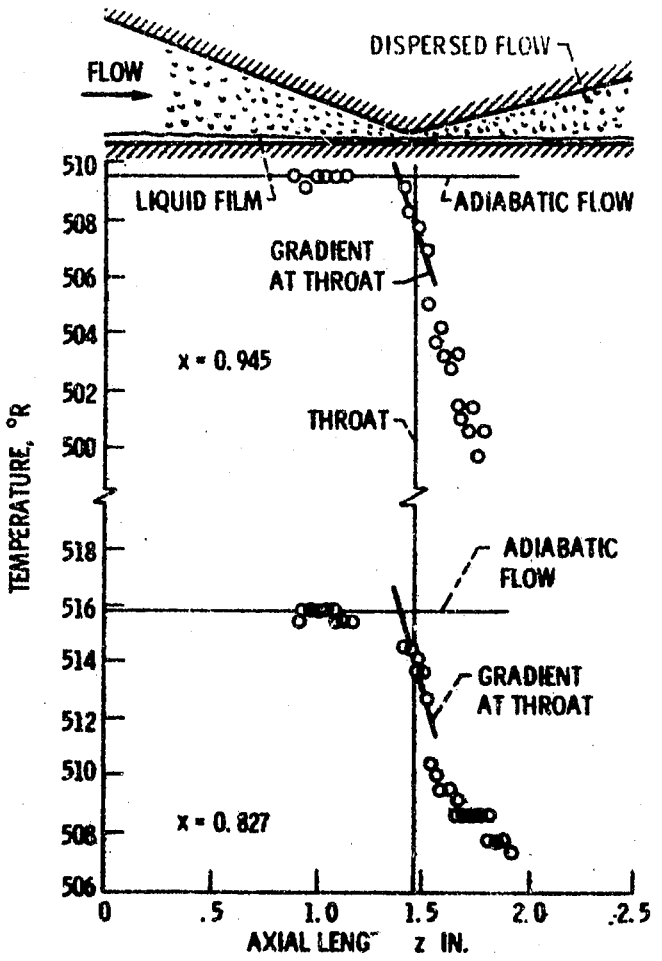

Figure 1. - Axial liquid film temperature profiles reported in Ref. 5.

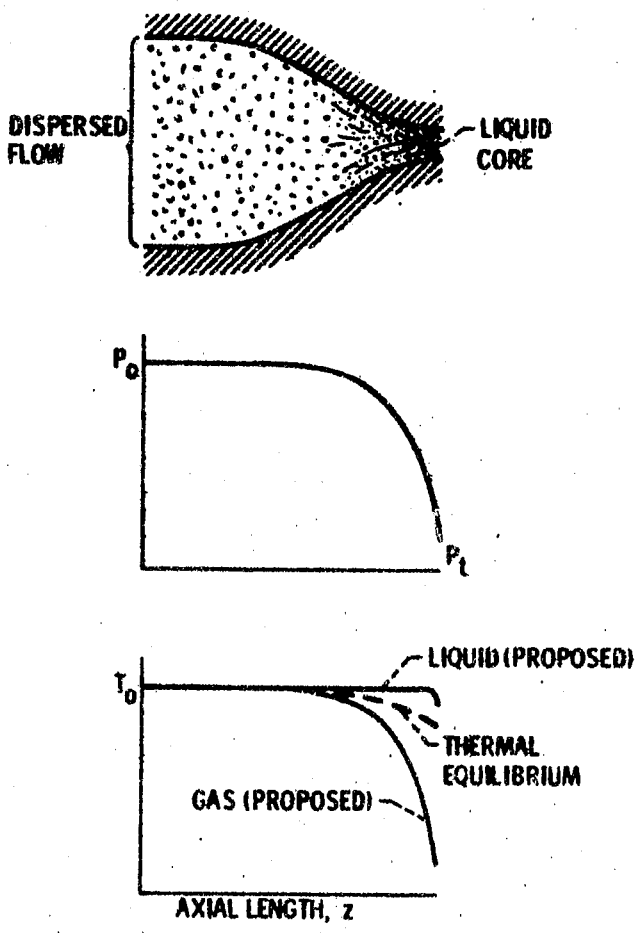

Figure 2. - Proposed flow pattern development and accompanying heat transfer behavior.

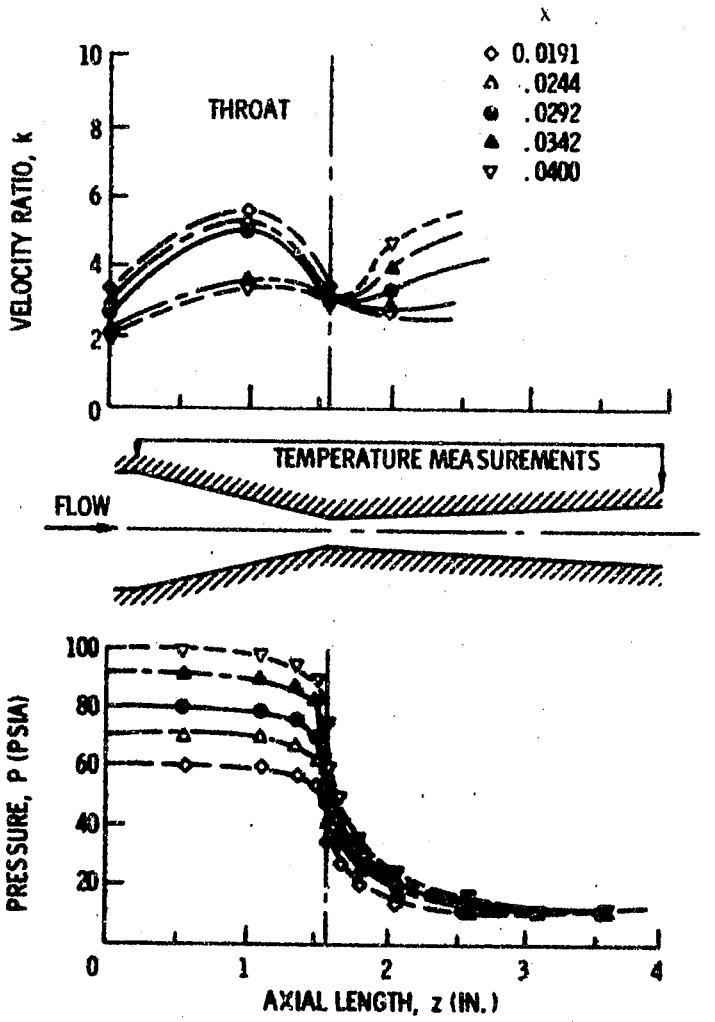

Figure 3. - Axial velocity ratio and pressure profiles for the data reported in Ref. 9.

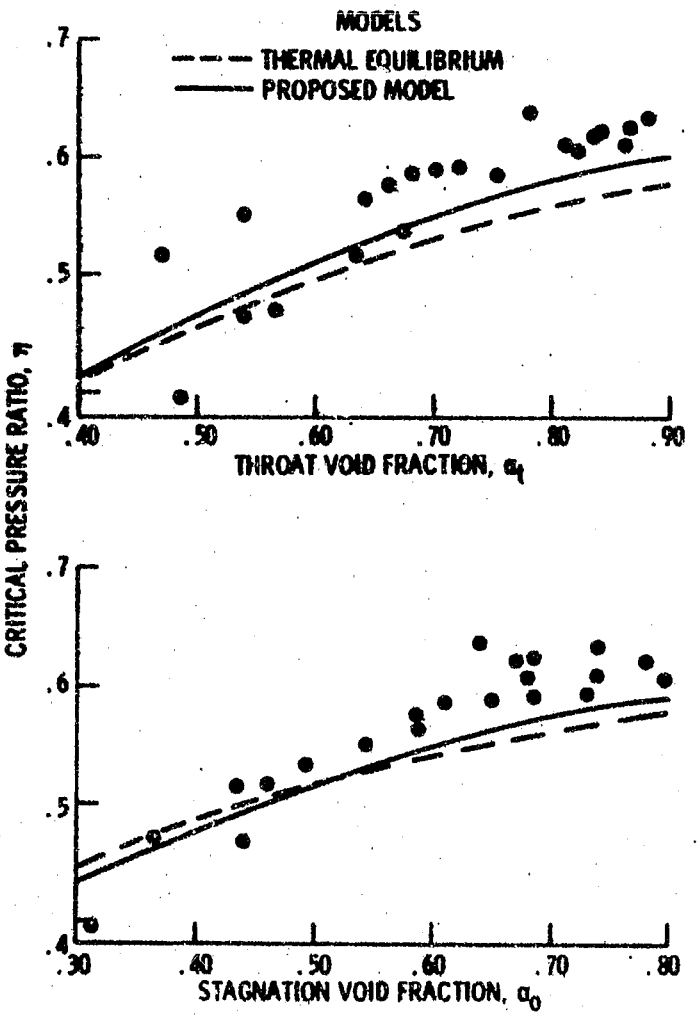

Figure 4. - Comparison of the proposed and thermal equilibrium critical pressure ratio predictions with the experimental data of Ref. 9.

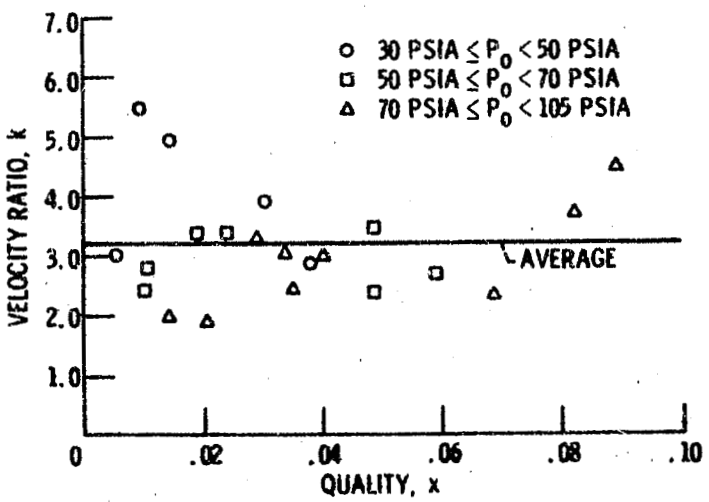

Figure 5. - Throat velocity ratios interpreted from the experimental results of Ref. 9.

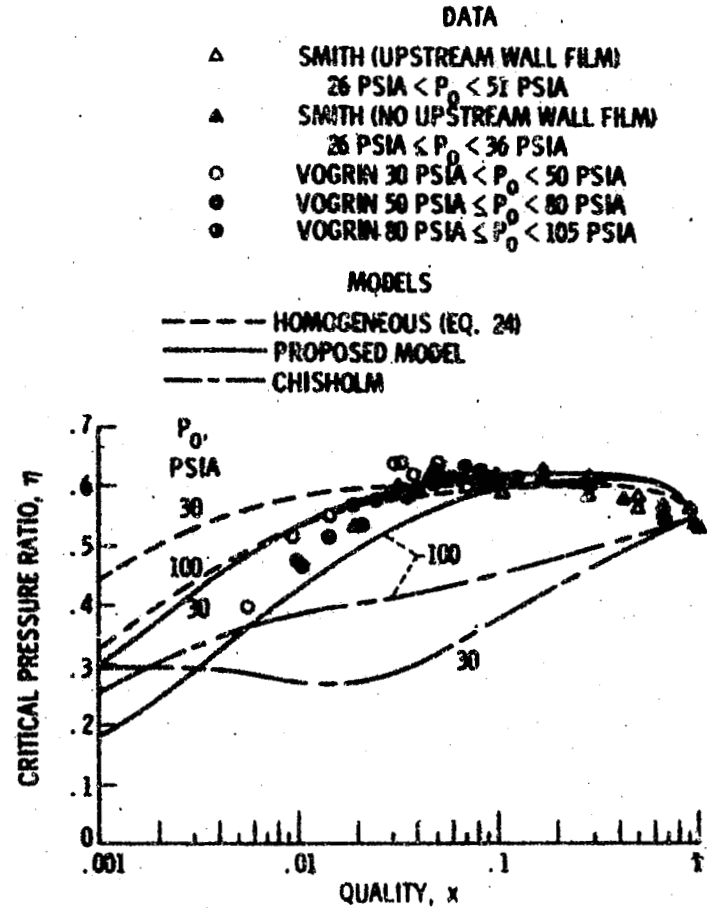

Figure 6. - Comparison of the critical pressure ratio predictions and the experimental results of Refs. 5 and 9.

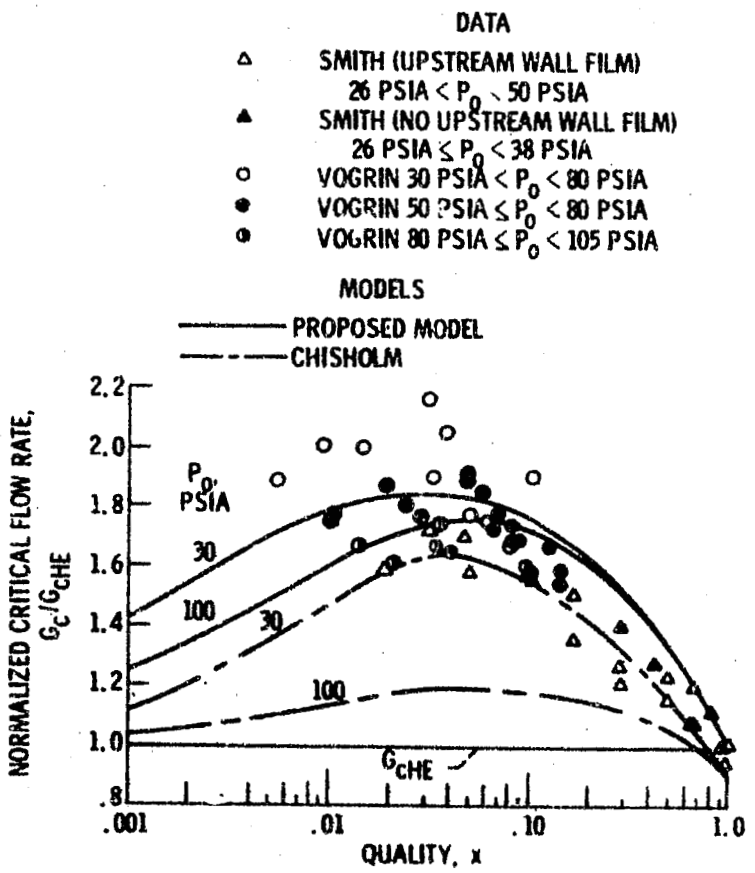

Figure 7. - A comparison of the critical flow predictions and the experimental results of Refs. 5 and 9.

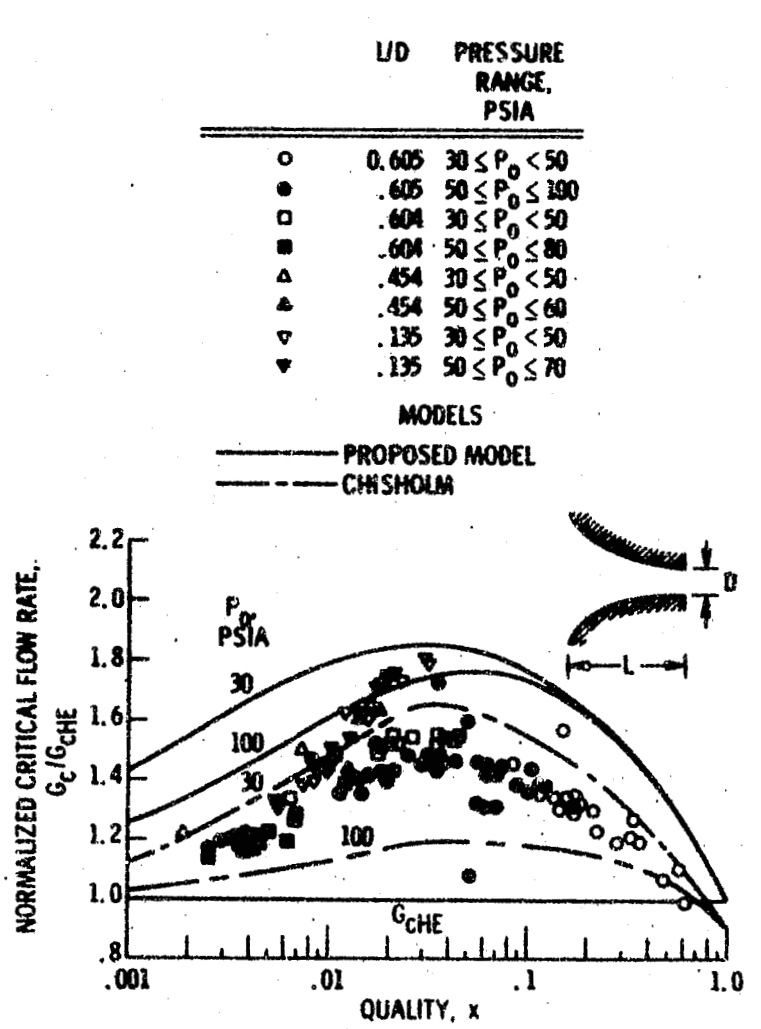

Figure 8. - A comparison of the critical flow rate prediction and the experimental results of Ref. 13.

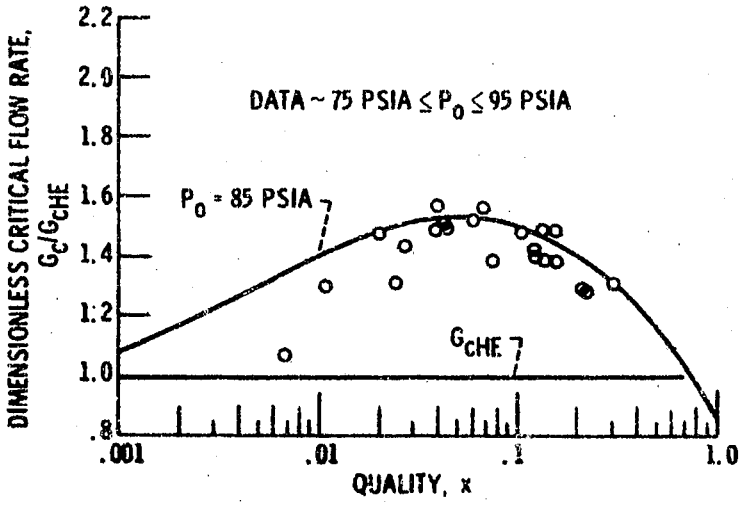

Figure 9. - A comparison between the orifice critical flow prediction and the experimental results of Ref. 13.

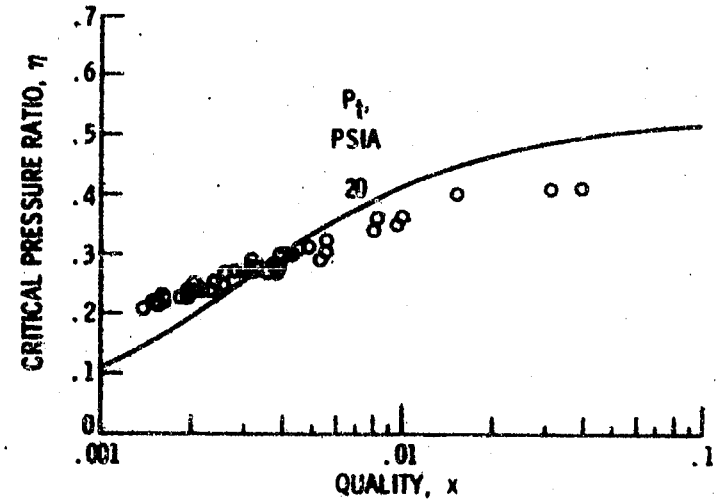

Figure 10. - A comparison of the critical pressure ratio prediction and the cylindrical nozzle data of Ref. 17.

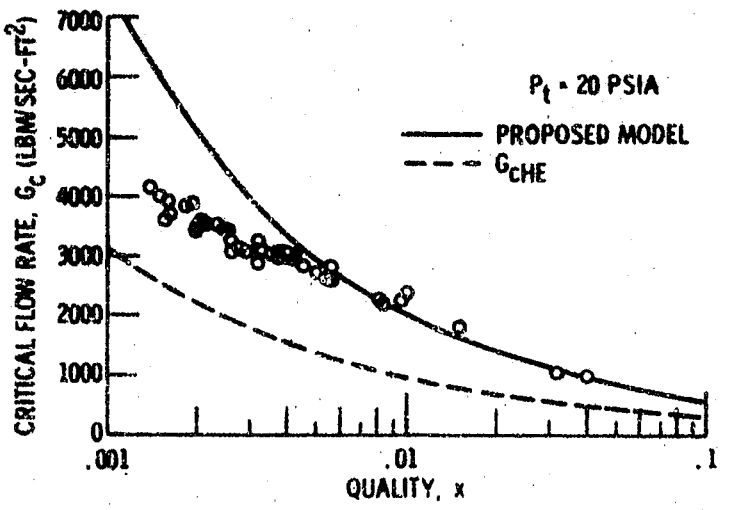

Figure 11. - A comparison between the critical flow prediction and the cylindrical nozzle data of Ref. 17.